Effects of Cholinergic Modulation on Spike Frequency Adaptation and Spike Timing

A.C. Tang A.M. Bartels T.J. Sejnowski

Abstract

Cholinergic neurons in the basal forebrain, which innervate all cortical regions [1], modulate neuronal excitability [2, 3] and influence learning and memory [4, 5, 6]. Cholinergic reduction of spike freqüency adaptation in cortical neurons in response to a square pulse input is considered an important mechanism for cholinergic control of neuronal excitability [2, 3, 7], the generation of theta rhythms [8, 9], and cholinergic modulation of higher level functions [10, 11]. We used whole cell patch clamp recordings in neocortical slices and computational simulations to show that, in contrast to the strong spike frequency adaptation observed with square pulse inputs, spike frequency adaptation was reduced or absent with fluctuating inputs that resemble in vivo *conditions [12]. Furthermore, unlike modulation of responses to square pulse inputs, displacement of spike times in response to fluctuating inputs following cholinergic modulation was less than three milliseconds, comparable to the spike jitter observed during visual stimulation under* in vivo *conditions [13]. These results suggest that cholinergic modulation is compatible with a neural code based on precise spike timing [14, 15, 16] but not a spike interval code, and that cholinergic mechanisms other than those involving adaptation [17, 18, 19] may contribute significantly to cholinergic modulation of learning and memory [20].*

We stimulated neocortical neurons in the rat visual cortex with both conventional square pulse inputs and fluctuating inputs that resembled the impact of synaptic inputs recorded *in vivo*. In previous studies using square pulse inputs, acetylcholine significantly enhanced the firing rate by blocking the currents underlying spike frequency adaptation [2, 3, 7] (Fig. 1a and 1c). Cholinergic reduction of adaption has also been linked to higher level processing through neural network models of learning and memory and theta wave generation [8, 9, 10, 11]. In contrast to the strong spike frequency adaptation evoked by a square pulse input (Fig. 1a), injection of a fluctuating current into neocortical neurons reduced or completely eliminated pronounced spike frequency adaptation (Fig. 1b). Adaptation measured within a block of 20 trials was high only when square pulse inputs were used and became much weaker for fluctuating inputs (cf. 2a and 2b control; paired t test, t=4.923, $p \leq .001$, N=10). Instead of a differential increase of excitability for the later period of stimulation due to a blockade of adaptation (Fig. 2a), cholinergic modulation increased the excitability more uniformly for the fluctuating input (Fig. 2b).

Does cholinergic modulation of adaptation contribute to cholinergic control of excitability in a manner that depends on the form of input? The increase in excitability and the

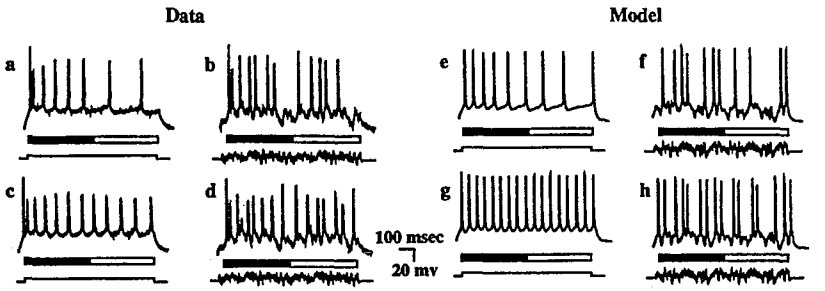

Figure 1: Cholinergic modulation of spike trains elicited by square pulse and fluctuating inputs in a neocortical neuron (a-d) and a model neuron (e-h). a, Strong spike frequency adaptation in response to 90 pA square pulse current injection (below). b, Reduced spike frequency adaptation in response to the fluctuating current injection (standard deviation of fluctuation: 72 pA; mean amplitude: 90 pA). The solid and white bars under the voltage traces mark the first and second halves of the total stimulus duration (900 ms). c, Cholinergic reduction of adaptation and non-uniform increase of excitability in response to the same input as in a (carbachol: 5 μM); d, Uniform increase of excitability due to cholinergic modulation in response to the same stimulus as in b. *e*, Model: Strong spike frequency adaptation in response to 150 pA square pulse current injection (below). *f*, Model: Reduced spike frequency adaptation in response to the fluctuating current injection (standard deviation of fluctuation: 150 pA, mean amplitude: 150 pA). *g*, Model: Simulated cholinergic reduction of adaptation and non-uniform increase of excitability in response to the same input as in *e*. *h*, Model: Uniform cholinergic increase of excitability in response to the same stimulus as in *f*.

reduction in adaptation induced by carbachol (5 μM) for the square pulse and fluctuating iputs are graphed in Fig. 2c. The lines connecting the control (origin) to the carbachol condition were less steep for the fluctuating inputs (filled circle) than for the square pulse inputs (open circle), indicating that reducing spike frequency adaptation became less effective in enhancing neuronal excitability when input fluctuations were increased ($p \leq .032$, N=5).

To show that the reduced adaptation due to increased stimulus fluctuation observed in the slice experiments is a general property of cortical neurons over a wide range of conditions, we constructed a model neuron that exhibited the basic response characteristics of neocortical neurons (Figs. 1, 2, and 4). In the model, spike frequency adaptation decreased as a function of increasing amplitude of stimulus fluctuation (Fig. 3a) for different levels of mean synaptic inputs, a range of initial degrees of adaptation, and a variety of model geometries. If reduction of adaptation contributes less to cholinergic control of excitability (Fig. 2c), then I_{AHP}, the primary current underlying adaptation [17] should correspondingly show less correlation with increasing excitability. Simulations at multiple levels of cholinergic reduction of I_{sAHP} produced less increase in neuronal excitability when the stimulus fluctuation was increased (Fig. 3b). The relatively uniform increase of excitability throughout the stimulation interval during fluctuating inputs suggests an important role for other potassium currents. This is supported by the simulations showing that modulation of I_{leak} and I_M significantly potentiated the effects of cholinergic modulation of I_{sAHP} on excitability (Fig. 4c and 4d). Although spike frequency adaptation induced by a square pulse input has been considered a powerful mechanism in mediating cholinergic enhancement of

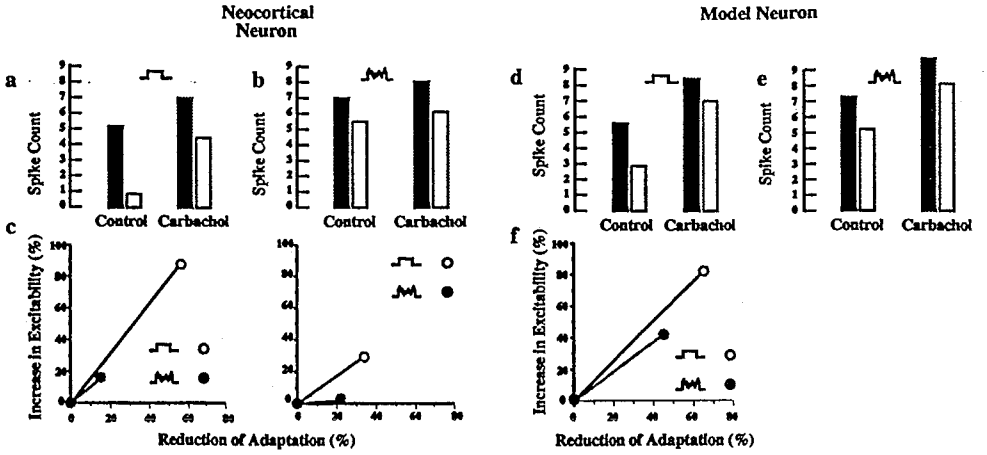

Figure 2: Effect of stimulus fluctuation on adaptation and effect of cholinergic modulation on the relationship between adaptation and excitability in neocortical (a-c) and model (d-f) neurons. For each condition shown in Fig. 1, the average spike count C1 during the first half (solid) and C2 the second half (white) of the stimulation (900 ms) are plotted in the bar graphs for a block of 20 trials. An adaptation index is defined as $A = (C1 - C2)/C1$. For the fluctuating input, the same random sequence was repeated during the first and second half of stimulus to insure fair comparison, and 20 different sequences were used. Carbachol = 5 μM for all panels. *a*, Square pulse input, control (mean±sem): A=83±4%. Carbachol: A=36±2%. *b*, Fluctuating input, control: A=26±2%. Carbachol: A=22±3%. *c*, Increase in excitability as a function of reduction of adaptation from two neurons (right and left) in response to carbachol for square pulse inputs (open circle) and fluctuating inputs (filled circle). For fluctuating inputs, carbachol was less effective in increasing the excitability for a given amount of reduction in adaptation compared to those for square pulse inputs, as judged by the shallower slope of the lines connecting the control (origin) to the carbachol conditions. The slope difference, the initial adaptation, and the absolute firing rate varied from cell to cell, some of which were strongly adapting; however for all cells examined, the slopes for fluctuating inputs were consistently smaller than for square pulse inputs. *d*, Model, square pulse inputs, control: A= 47±3%. Carbachol: A=16±2%. *e*, Model, fluctuating inputs, control: A= 27±3%. Carbachol: A=13±2%. *f*, The model neuron also had a smaller slope for fluctuating inputs than for square pulse inputs.

neuronal excitability [2, 3], the reduction or lack of adaptation observed with the fluctuating inputs (which should be even less influential at 37°C[23]), suggests that the contribution of spike frequency adaptation to normal function and to cholinergic control of excitability *in vivo* needs to be reconsidered. The decreased impact of I_{AHP} and the strong interaction among multiple potassium currents under fluctuating inputs suggests that other cholinergic mechanisms, such as a reduction in leak potassium or M currents [17, 19], or selective suppression of recurrent synaptic transmission [18] should be included in formulating theories on cellular basis of learning and memory and in designing drugs that alleviate cognitive deficits.

The effects of cholinergic modulation observed with fluctuating stimuli have implications for the possibility of temporal coding in the neocortex [14, 15, 16, 24]. The preservation of spike timing suggests that although acetylcholine enhances neuronal excitability, a stable code based on spike-timing can be maintained under varying concentrations of neuromod-

ulators, contrary to previous expectations based on conventional square pulse inputs. By probing neurons with stimuli resembling *in vivo* conditions, it may be possible to uncover other emergent properties and create new links between cellular mechanisms and higher level cognitive functions.

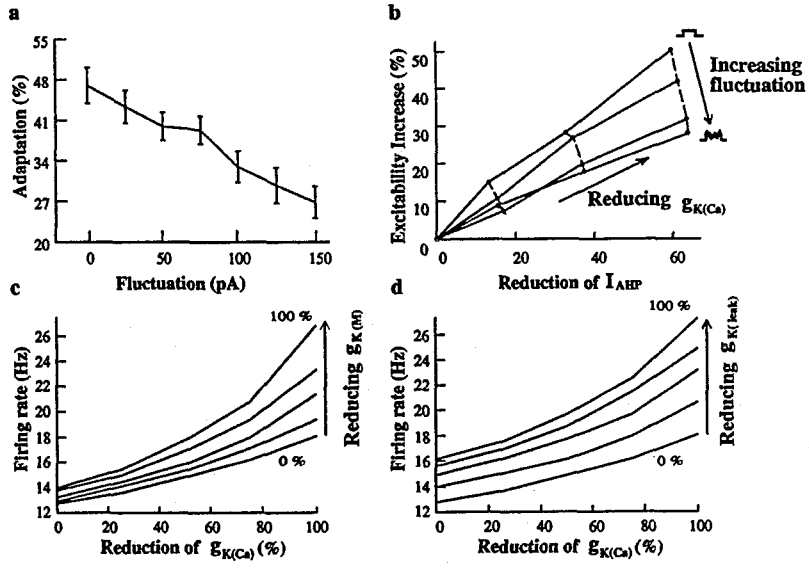

Figure 3: Simulation results on adaptation and cholinergic control of excitability from a model cortical neuron. *a*, Adaptation decreases as a function of stimulus fluctuation. N = 20 trials (20 seeds) per condition. Similar results were also obtained for (1) more strongly adapting cells with very large values of the slow calcium dependent potassium conductance $g_{K(Ca)}$ (0.2 to 1.6 pS/μm^2, shown for 0.8 pS/μm^2); (2) Mean current injection from 100 pA to 300 pA, shown for 150 pA. (3) 10 and 1 compartment layer 2/3 pyramidal cell models, shown for the 10-compartment model. *b*, Increased excitability as a function of reduction in I_{sAHP}. The solid lines represent different levels of stimulus fluctuation. The slope decreases as stimulus fluctuation increases (from 0, 50, 100 to 150 pA), indicating that reducing I_{sAHP} becomes less effective in enhancing excitability as input fluctuation increases. To simulate the primary carbachol effect, $g_{K(Ca)}$ was set to 0.8, 0.6, 0.4, and 0.2 pS/μm^2 respectively for control (origin) and increasing carbachol concentrations (successive points on the solid line). *c and d*, Modulation of other potassium currents potentiate the effect of I_{sAHP} modulation on cholinergic control of excitability. In the absence of I_M and I_{leak} modulation, complete blockade of I_{sAHP} increased the firing rate from 13 to 18 Hz. *c*, Accompanied by a complete I_M blockade, the effect of I_{sAHP} modulation almost doubled (14 to 27 Hz). *d*, Accompanied by a modulation of I_{leak}, associated with an increase in resting membrane potential by 10 mV, the effects of I_{sAHP} modulation increased by a half (16 to 27 Hz).

A cortical neuron is generally thought to carry information in its average rate of spiking, but the timing of individual spikes may also be important [21, 14, 15, 16, 22] Since neurons function in a dynamic neuromodulatory environment, the code used by the nervous system must be stable during changes in neuromodulator concentrations. Modification of spike timing, implied by cholinergic reduction in spike frequency adaptation to a square pulse input (Fig. 4a), might disrupt information conveyed by spike times. However, in the presence of carbachol, the timing of the spikes, but not interspike intervals, was preserved to the same fluctuating inputs, despite an increase in excitability due to the insertion of

additional spikes (Fig. 4b). Cholinergic preservation of spike timing between the control and carbachol conditions is indicated by the minimal displacement of spikes shown in the smoothed histograms (Fig. 4c). The mean spike displacement for carbachol concentrations of 5 μM and 7.5 μM was 2.76±0.38 ms (N=14), less than the minimum spike jitter of 3 to 5 ms reported *in vivo* for visual cortex [13].

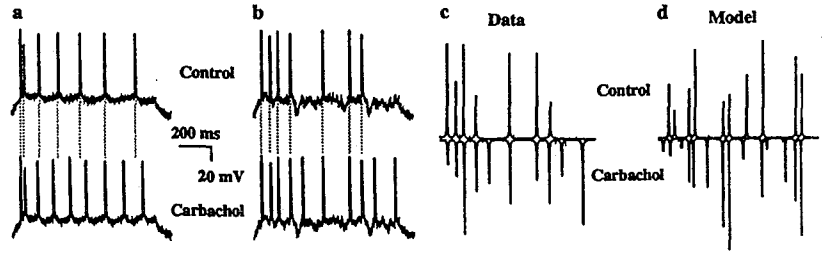

Figure 4: Cholinergic modulation preserved spike timing in response to the same fluctuating input. *a*, Cholinergic reduction of spike frequency adaptation to constant input for a neocortical neuron. The gray vertical lines show the timing of spike initiation under the control condition. Misalignment to the carbachol condition indicates a modification of spike timing. *b*, Cholinergic modulation preserved spike timing and enhanced excitability by inserting additional spikes for the fluctuating input condition. *c*, Preservation of spike timing for fluctuating inputs shown in smoothed histograms (20 trials), comparing control (above) and carbachol (inverted) in the same neuron. *d*, Preservation of spike timing for fluctuating inputs in the model neuron. The displacement in spike timing for each event (see [14]) in the histogram, d_i, is defined as the time difference between the nearest peaks of the events under carbachol and control conditions. The weight for each event, w_i, is determined by the height of the event (the greater the height, the less the spike jitter). Define mean displacement, $D = \sum d_i w_i / \sum w_i$, where $i = 1, 2, ...$ is the event index in the control condition. For each cell, D was measured using identical fluctuating input. For 5 and 7.5 μM carbachol (mean±sem): 2.76±.38 ms, N=15; for 15 μM carbachol: D=3.33 ms, N=1; for 30 μM carbachol: D=9.3 ms, N=2. For all 18 cells examined, the range of mean current injection is from 50 to 120 pA; standard deviation of current fluctuation from 50 to 100 pA. The spike jitter, measured as the mean half width of the events, under repeated identical stimulation was not changed significantly by carbachol (standard deviation for control (mean±sem) was 0.9±0.3ms and for the carbachol condition was 0.9±0.4 ms).

Methods

Experimental: Coronal slices of 400 μm were prepared from 14 to 18 days old Long Evans rats. Using the whole cell patch-clamp technique, somatic recordings were obtained under current clamp from 30 neocortical neurons in the rat visual cortex under room temperature (23°C). Resting potential = -64.1±1.07 (mean±sem); input resistance = 221±30 (mean±sem). The patch pipet contains (in mM): 100 KGluconate, 25 KCl, 5 NaCl, 0.2 EGTA, 10.0 HEPES, 4.0 ATP-Mg and 0.3 GTP-Li. External solution contains (in mM): 126 NaCl, 1.25 NaH_2PO_4, 10.0 D-glucose, 2.50 KCl, 2.00 $MgCl_2$, 2.00 $CaCl_2$. Data were taken at the mid-portion of the neuron's total dynamic range to avoid ceiling effect. The cholinergic agonist carbachol at concentrations of 5, 7.5, 15, 30 μM was delivered through bath perfusion (perfusion time: between 1 and 20 min). For each cell, three sets of blocks were recorded before, during and after carbachol perfusion at a given concentration. Each block contained 20 trials of stimulation under identical experimental conditions. To generate the fluctuating input, filtered Gaussian noise of zero mean was added to square pulse

inputs [14, 25]. The Gaussian noise signal was convolved with an alpha function with a time constant of 3 ms [14], chosen to reflect the time course of the synaptic events. Current fluctuation were no greater than 80% of the mean input and resulted in a subthreshold membrane potential fluctuation comparable to those recorded under *in vivo* whole cell patch-clamp [12].

Simulation: Simulations were performed on a reduced 8 compartment model [26], based on a reconstructed layer 2 pyramidal cell [27] (data shown) and on a one compartment model (data not shown) using the simulator NEURON [28]. An axon hillock and initial segment comprising two additional compartments taken from [29] were added to the 8 compartment model. The models were constrained by the basic response characteristics of experimentally recorded neocortical neurons shown in Figs. 1, 2, and 4. (1) *Model parameters*: Calcium dependency of the $g_{K(Ca)}$ and its channel density were modeled to reproduce the recorded spike trains under control and carbachol conditions. The implementation of the currents were the same as in [30] with following exceptions. Specific rate functions: fast sodium current, I_{Na}: half-activation voltages were shifted by -5mV; slow non-inactivating potassium current, I_{K_M}: $\alpha = 10^{-3}(v+35)/(1-e^{-(v+35)/9})$, $\beta = -10^{-3}(v+35)/(1-e^{(v+35)/9})$; high voltage activated calcium current, I_{Ca} inactivation : $\alpha = 4.57 \cdot 10^{-4} e^{-(v+13)/50}$, $\beta = 0.001/(1+e^{-(v+15)/28})$; the slow calcium dependent potassium current, I_{sAHP}: $\alpha([Ca^{++}]_i) = 500([Ca_i^{++}]^2 - [Ca^{++}]_\infty^2)$, $\beta = 0.001$. Calcium removal: $d[Ca_i^{++}]/dt = -10^5 I_{Ca}/2F - ([Ca_i^{++}] - [Ca_\infty^{++}])/\tau$, where τ =127 ms, and $[Ca_\infty^{++}] = 50$ nM. Specific capacitance $C_m = 1\mu F/\mu m^2$, specific membrane resistance R_m =40 KΩcm^2, specific axial resistance R_a =200 Ωcm, membrane resting potential $-70mV$. Channel densities (in pS/μm^2) were as follows. Multicompartment model: Dendrites: $g_{Na} = 30$; $g_{Ca} = 0.1$; $g_{K(Ca)} = 0.8$, $g_{K_M} = 0.25$, fast potassium delayed rectifier: $g_{K_\nu} = 0.5$. Soma: except $g_{K_\nu} = 6$ same as dendrites. Axon hillock and initial segment: $g_{Na} = 30,000$ and $g_{K_\nu} = 700$. The dendritic passive and active properties except R_a were scaled by a factor of 3 to compensate for the reduction of surface area due to the reduction method [26]. One compartment model: $g_{Na} = 400$, $g_{K_\nu} = 4$, $g_{Ca} = 0.1$; $g_{K(Ca)} = 2.8$, (no g_{K_M}). Other properties as in the multicompartment model. Temperature: 23°C. (2) *Cholinergic modulation*: We simulated the effects of carbachol by reducing three potassium conductances, $g_{K(Ca)}$, g_{K_M}, and $g_{K,leak}$, underlying the I_{sAHP}, I_M, and $I_{K_{leak}}$ respectively [31]. The primary carbachol effects were simulated by a 75% reduction in $g_{K(Ca)}$, 12.5% reduction in g_{K_M}, and 12.5% reduction in $g_{K_{leak}}$. The amount of reduction of g_{K_M} was derived from the measured ratio of reduction of $g_{K(Ca)}/g_{K_M}$ in hippocampal pyramidal cells [17]. The reduction of $g_{K_{leak}}$ corresponds to a depolarization of 2.5 mV.

Stimulus parameter: Intrinsic noise was simulated by injecting fluctuating currents (standard deviation: 10 pA) to fit the spike jitter observed experimentally. The mean current injection in data shown here was 150 pA, and the fluctuation had a standard deviation of 150 pA, leading to subthreshold membrane potential fluctuations comparable to those in the experimental data. Correspondence and requests for materials to tang@salk.edu.

Acknowledgments Research supported by the Howard Hughes Medical Institute, the National Institutes of Health, and Schweizerische Studienstiftung. We thank Zachary Mainen, Barak Pearlmutter, Raphael Ritz, Kechen Zhang, Anthony Zador, Brian Christie, David Horn, and Bartlett Mel for their critical comments and helpful discussions.

References

[1] M. Marsel Mesulam. The cholinergic contribution to neuromodulation in the cerebral cortex. *Seminar in Neurosciences*, 7:297–307, 1995.

[2] D. A. McCormick. Actions of acetylecholine in the cerebral cortex and thalamus and implications for function. *Prog. Brain Res.*, 98:303–308, 1993.

[3] R.A. Nicoll. The coupling of neurotransmitter receptors to ion channels in the brain. *Science*, 241:545–550, 1988.

[4] J. Winkler, S.T. Suhr, F.H. Gage, L.J. Thal, and L.J. Fisher. Essential role of neocortical acetylcholine in spatial memory. *Nature*, 375:484–487, 1995.

[5] H. C. Fibiger. Cholinergic mechanisms in learning, memory and dementia: a review of recent evidence. *Trends Neurosci.*, 6:220–223, 1991.

[6] J.J. Hagan and R.G.M. Morris. The cholinergic hypothesis of memory: a review of animal experiments. In L.L. Iversen, S.D. Iversen, and S.H. Snyder, editors, *Psychopharmacology of the aging nervous system*, pages 237–324. Plenum Press, New York, 1989.

[7] D. A. McCormick and A. Williamson. Convergence and divergence of neurotransmitter action in human cerebral cortex. *Proc. Natl. Acad. Sci*, 86:8098–8102, 1989.

[8] H. Liljenstrom and M.E. Hasselmo. Cholinergic modulation of cortical oscillatory dynamics. *J. Neurophy.*, 74(1):288–297, 1995.

[9] R.D. Traub, R. Miles, and G. Buzsaki. Computer simulation of carbachol-driven rhythmic population oscillation in the CA3 region of the *in vitro* rat hippocampus. *J. Neurophy.*, 451:653–672, 1992.

[10] E. Barkai and M. E. Hasselmo. Modulation of the inputoutput function of rat piriform cortex pyramidal cells. *J. Neurophysiol.*, 72:644–658, 1994.

[11] Edi Barkai, Ross E. Bergman, Gregory Horwitz, and M. E. Hasselmo. Modulation of associative memory function in a biophysical simulation of rat piriform cortex. *J. Neurophysiol.*, 72:659–677, 1994.

[12] D. Ferster and B. Jagadeesh. EPSP-IPSP interactions in cat visual cortex studied with *in vivo* whole-cell patch recording. *J. Neurosci.*, 12(4):1262–1274, 1992.

[13] W. Bair and C. Koch. Temporal precision of spike trains in extrastriate cortex of the behaving macaque monkey. *Neural Computation*, 8(6):1184–1202, 1996.

[14] Z. F. Mainen and T. J. Sejnowski. Reliability of spike timing in neocortical neurons. *Science*, 268:1503–6, 1995.

[15] R.C. deCharms and M.M. Merzenich. Primary cortical representation of sounds by the coordination of action-potential timing. *Nature*, 381:610–3, 1996.

[16] M. Abeles, H. Bergman, E. Margalit, and E Vaadia. Spatiotemporal firing patterns in the frontal cortex of behaving monkeys. *J. Neurophysiol.*, 70:1629–1638, 1993.

[17] D. V. Madison, B. Lancaster, and R. A. Nicoll. Voltage clamp analysis of cholinergic action in the hippocampus. *J. Neurosci.*, 7(3):733–741, 1987.

[18] M. E. Hasselmo and J. M. Bower. Cholinergic suppression specific to intrinsic not afferent fiber synapses in rat piriform (olfactory) cortex. *J. Neurophysiol.*, 67(5):1222–1229, 1992.

[19] K. Krnjevic, R. Purain, and L. Renaud. The mechanism of excitation of acetylcholine in the cerebral cortex. *J. Physiol.*, 215:447–465, 1971.

[20] M. E. Hasselmo and J. M. Bower. Acetylcholine and memory. *Trends Neurosci.*, 16(6):218–222, 1993.

[21] F. Rieke, D. Warland, R. de Ruyter van Steveninck, and W. Bialek. *Spikes: Exploring the Neural Code.* MIT Press, 1996.

[22] John J. Hopfield. Pattern recognition computation using action potential timing for stimulus representation. *Nature*, 376:33–36, 1995.

[23] S.M. Thompson, L.M Masukawa, and D.A. Prince. Temperature dependence of intrinsic membrane properties and synaptic potentials in hippocampal ca1 neurons in vitro. *J. Neurosci.*, 5(3):817–24, 1985.

[24] B.J. Richmond, L.M. Optican, M. Podel, and H. Spitzer. Temporal encoding of two-dimensional patterns by single units in the primate inferior temporal cortex. i. response characteristics. *J. Neurophysiol.*, 57:132–146, 1987.

[25] H.L. Bryant and J.P Segundo. Spike initiation by transmembrane current: A white-noise analysis. *J. Physiol.*, 260:279–314, 1976.

[26] P. C. Bush and T. J. Sejnowski. Reduced compartmental models of neocortical pyramidal cells. *J. Neurosci. Method.*, 46:159–166, 1993.

[27] C. Koch, R. Douglas, and U. Wehmeier. Visibility of synaptically induced conductance changes: theory and simulations of anatomically characterized cortical pyramidal cells. *J. Neurosci.*, 10:1728–1744, 1990.

[28] M. Hines. A program for simulation of nerve equations. In F.H. Eeckman, editor, *Neural Systems: Analysis and Modeling*, pages 127–136. Kluwer Academic Publishers, Boston, MA, 1993.

[29] Z. F. Mainen, J. Joerges, J.R. Huguenard, and T. J. Sejnowski. A model of spike initiation in neocortical pyramidal neurons. *Neuron*, 15:1427–1439, 1995.

[30] Z. F. Mainen and T. J. Sejnowski. Influence of dendritic structure on firing pattern in model neocortical neurons. *Nature*, 382:363–6, 1996.

[31] D. V. Madison and R. A. Nicoll. Control of the repetitive discharge of rat CA1 pyramidal neurons in vitro. *J. Physiol.*, 354:319–331, 1984.